

Thermalization and localization of an oscillating Bose-Einstein condensate in a disordered trapChe-Hsiu Hsueh,¹ Russell Ong,¹ Jing-Fu Tseng,¹ Makoto Tsubota,^{2,3,*} and Wen-Chin Wu^{1,†}¹*Department of Physics, National Taiwan Normal University, Taipei 11677, Taiwan*²*Department of Physics, Osaka City University, Sugimoto 3-3-138, Sumiyoshi-ku, Osaka 558-8585, Japan*³*The OCU Advanced Research Institute for Natural Science and Technology (OCARINA), Osaka 558-8585, Japan*

(Received 27 July 2018; published 10 December 2018)

We numerically simulate an oscillating Bose-Einstein condensate in a disordered trap [Phys. Rev. A **82**, 033603 (2010)] and the results are in good agreement with the experiment. It shows that the disorder acts as a medium, which results in a relaxation from nonequilibrium to equilibrium, i.e., thermalization. An algebraic localization is realized when the system approaches the equilibrium, and if the system falls into the regime when the healing length of the condensate exceeds the correlation length of the disorder, exponential Anderson localization is to be observed.

DOI: [10.1103/PhysRevA.98.063613](https://doi.org/10.1103/PhysRevA.98.063613)

Anderson localization (AL) had been a long-studied phenomenon in electronic systems [1]. When transporting in an environment with random disorder, waves of electrons get localized after multiple scattering with the disorder. Recently there has been a resurgence of studies of AL in a variety of systems such as photonic crystals [2,3], ultrasound in 3D elastic networks [4], quantum chaotic systems [5], and cold atoms [6,7]. The experiment [6] of cold atoms was done by expanding Bose condensate in a weak random potential in which the initial healing length (ξ) of the condensate exceeds the correlation length (σ_D) of the disorder, $\xi > \sigma_D$. The experiment [6] confirmed that the localized condensate exhibits an *exponential* density profile in a one-dimensional geometry, in agreement with the theory of Sanchez-Palencia *et al.* [8].

In this paper, we show that an oscillating condensate in a disordered trap, such as the experiment done by Dries *et al.* [9], can also exhibit AL when it comes to equilibrium and if it falls into the regime $\xi > \sigma_D$. Using exactly the same parameters of the experiment reported in Fig. 2 of Ref. [9] for $\xi < \sigma_D$, we perform a numerical simulation based on the Gross-Pitavskii (GP) approach in the presence of a spatially random disorder potential. The results are in good agreement with the experiment. It allows us to verify that when it passes an onset time t_c (discussed later), the system enters an *algebraical* localized state [8]. This motivates us to carry out another simulation with the same parameters except by reducing σ_D to make $\xi > \sigma_D$. In this case, exponential AL is eventually observed.

Another important factor in such a system is that it provides a simple framework to investigate the long-standing question on how an “isolated” many-body quantum system, without coupling to the reservoir, can relax to a steady state that seems to be in thermodynamic equilibrium, i.e.,

thermalization [10–12]. The temporal entropy reveals that a relaxation process from nonequilibrium to equilibrium does exist. Random disorder plays the role of a *medium* (or *transistor*) which results in the exchange of partial kinetic energy with partial potential energy. Both kinetic and potential energies come to a constant when the system reaches the thermodynamic equilibrium. There is no dissipation of the total energy through any kind of *friction*. The results also suggest that the system thermalizes first, and when thermalization has occurred, localization establishes itself in a second stage.

To make a direct comparison with the experiment reported in Fig. 2 of Ref. [9], we consider a one-dimensional (1D) Bose gas with a repulsive contact interaction that is trapped in a harmonic potential $V_{ho}(z) = m\omega^2 z^2/2$. In the dilute and ultracold condition, the condensate wave function $\psi(z, t)$ is governed by the GP equation in the presence of a real spatially random disordered potential $V_{dis}(z)$,

$$i\hbar\partial_t\psi = \left[-\frac{\hbar^2}{2m}\partial_z^2 + V_{ho}(z) + V_{dis}(z) + Ng|\psi|^2 - \mu \right] \psi. \quad (1)$$

Here N is the total number of atoms, g is the coupling constant of contact interaction, μ is the chemical potential, and ψ is normalized to 1, $\int |\psi|^2 dz = 1$. The initial healing length at the center of the condensate is defined as $\xi = \hbar/\sqrt{2m\mu}$. The disorder correlation length σ_D is defined by fitting the autocorrelation function $\langle V_{dis}(z)V_{dis}(z + \Delta z) \rangle = V_D^2 \exp(-2\Delta z^2/\sigma_D^2)$ with V_D the strength of $V_{dis}(z)$ [13].

In the experiment, the condensate is released at a position off the center of the harmonic trap that results in the subsequent oscillations. For numerical convenience, we take an alternative scheme such that the condensate is released at the trap center but with an initial velocity v_0 . To obtain an initial wave function with a velocity v_0 , we apply the Galilean transformation $\psi = \varphi \exp(imv_0z)$ and the corresponding GP equation for the residual wave

*tsubota@sci.osaka-cu.ac.jp

†wu@ntnu.edu.tw

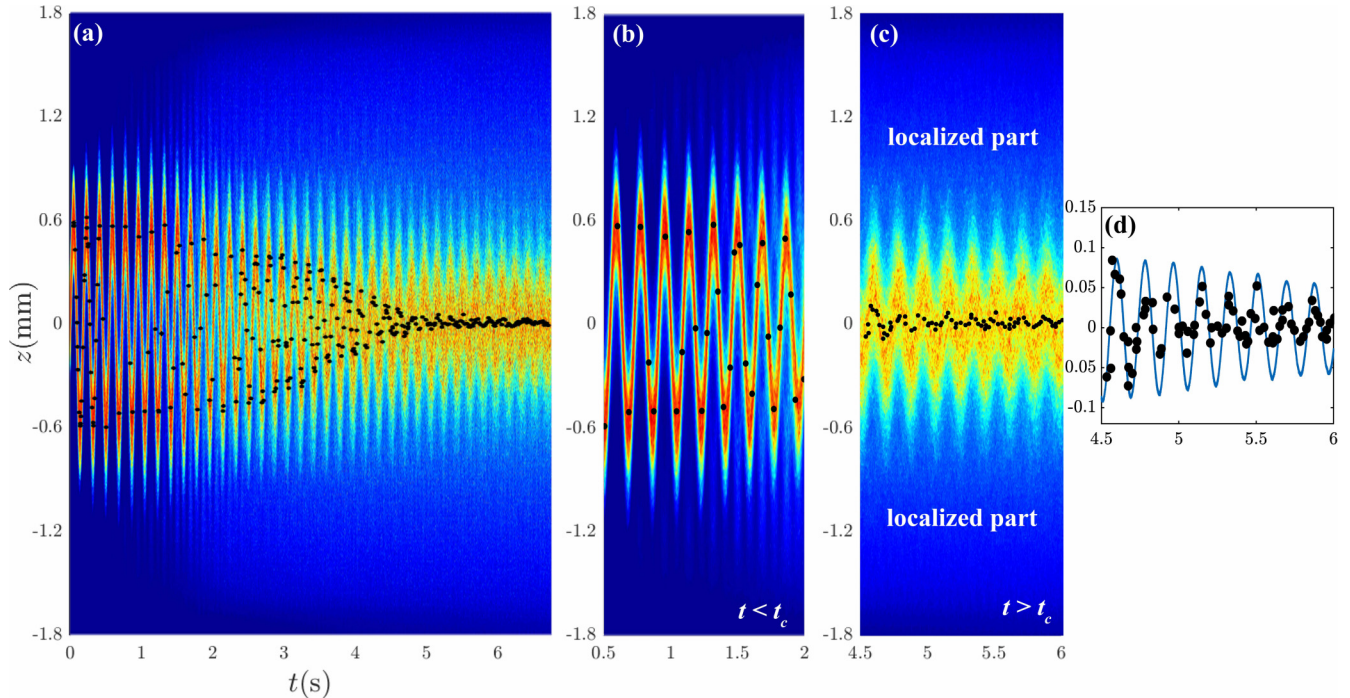


FIG. 1. (a) Spatial and temporal distribution of an oscillating condensate. The calculated norm of the spatial condensate wave function is potted in z direction at various times. Black dots are the experimentally measured temporal center-of-mass coordinates, taken from Fig. 2 of Ref. [9]. (b),(c) Close examinations of the results for $t < t_c \sim 4$ s and for $t > t_c$. (d) Blue line corresponds to the temporal center-of-mass positions calculated from the numerical results in (c).

function φ is

$$i\hbar\partial_t\varphi = \left[\frac{1}{2m} \left(\frac{\hbar}{i}\partial_z - mv_0 \right)^2 + V_{\text{ho}}(z) + V_{\text{dis}}(z) + Ng|\varphi|^2 - \mu \right] \varphi. \quad (2)$$

Long-term imaginary-time evolution of Eq. (2) gives φ which in turn gives the initial wave function ψ . A cutoff wave vector k_c corresponding to the shortest length scale or the largest k scale in association with the healing length ξ is naturally introduced in the simulation which gives the best results. In natural units $\hbar = m = \omega = 1$, experimental parameters are $\mu = 200$, $\xi = 0.05$, $v_0 = 37.5$, $V_D = 50.9$, and $\sigma_D = 0.25$ [9].

Figure 1(a) shows the spatial and temporal results of the oscillating condensate simulation. We plot, at various times, the calculated norm of the spatial condensate wave function in the z direction. For comparison, black dots correspond to experimentally measured temporal center-of-mass coordinates (reported in Fig. 2 of Ref. [9]). Surprisingly it gives a very good agreement between the simulation and the experiment. Close examinations of the results are shown in Fig. 1(b) for $t < t_c \sim 4$ s and in Fig. 1(c) for $t > t_c$. In view of Fig. 1(b), the calculated temporal density maxima match well with the experimental data points. One also sees that a minor (long-tail) part of atoms oscillate out of phase to the major (central) part of atoms, which is consistent with the experimental observation (see, for example, Fig. 5 in Ref. [9]).

In the experiment [9], the system was considered to be separated into a thermal (noncondensed) component and a condensed component which can be measured by different probes. The condensed component can be referred to as the coherent condensate, while the thermal or noncondensed component can be referred to as the incoherent noncondensate. However, in our simulations based on the GPE framework, no important incoherent component is generated. The result is consistent with the conclusion made in the paper of Clément *et al.* [14]. Therefore, we reproduce the experimental observations using a fully coherent theory. The central part of the condensate is weakly affected by the disorder, while the tails are subjected to multiple scattering and localization.

Figure 1(c) shows the regime when the system is approaching the equilibrium and the vast localization has occurred ($t > t_c$). At first glance, the calculated oscillations shown in Fig. 1(c) seem to be much stronger than the experimental data. To verify whether a good agreement is achieved between experiment and simulation, Fig. 1(d) plots the temporal center-of-mass positions calculated from the numerical results in Fig. 1(c). As seen, reasonably good agreement between experiment and simulation is also attained in this regime. In this regime, the system is seen to consist of both localized and extended parts—the localized part mainly exists in the long-tail area and the extended part mainly exists in the central area [15]. One sees that the oscillations of the central extended parts are significantly reduced compared to those at $t < t_c$. It signals that the system is approaching the equilibrium. In contrast, the long-tail part is seen to be completely static as the clear evidence of localization.

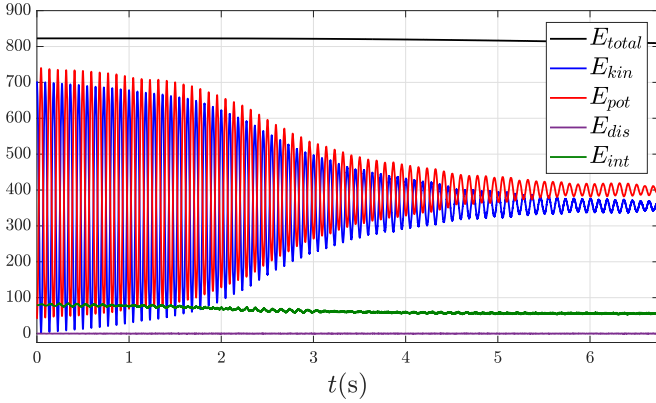


FIG. 2. Time evolution of the four energies (in units of $\hbar\omega$) in association with the dynamics shown in Fig. 1. Total energy is conserved for the entire process. The equilibrium temperature T_{eq} can be extracted from $E_{\text{kin}}(t \rightarrow \infty) \equiv k_B T_{\text{eq}}/2 \simeq 364\hbar\omega$ that yields $T_{\text{eq}} \simeq 192$ nK.

The good agreement between the simulation and the experiment allows us to study in more detail the two important phenomena, *thermalization* and *localization*. The total energy of the system consists of four terms: $E_{\text{tot}}(t) = E_{\text{kin}}(t) + E_{\text{pot}}(t) + E_{\text{dis}}(t) + E_{\text{int}}(t)$, where the kinetic energy $E_{\text{kin}}(t) = \int |\hbar\partial_z\psi|^2/(2m)dz$, the potential energy $E_{\text{pot}}(t) = \int V_{\text{ho}}|\psi|^2 dz$, the disorder energy $E_{\text{dis}}(t) = \int V_{\text{dis}}|\psi|^2 dz$, and the interaction energy $E_{\text{int}}(t) = (Ng/2) \int |\psi|^4 dz$. Figure 2 shows the time evolution of the four energies, respectively. As random disorder potential is rapidly varying in space, $E_{\text{dis}} \simeq 0$ (purple line) for the entire process. Moreover, because both the trapping and disorder potentials are real and time independent, one expects that there is no energy loss. Conservation of total energy is indeed confirmed in Fig. 2 (black line). Of most interest, during the process partial kinetic energy is in exchange with partial potential energy and when $t \gg t_c$, both energies are expected to come to a constant. It seems that the dissipation discussed in Refs. [9,16,17] can be realized as the result of the exchange between kinetic and potential energies.

In the current oscillating system with a large initial velocity, E_{int} is relatively small compared to both E_{kin} and E_{pot} . Thus the energy exchange occurs mainly between E_{kin} and E_{pot} . Moreover, as clearly seen in Fig. 2, the energy exchange rate or the transportation of the condensate is significantly reduced when $t > t_c$. One can also verify whether the virial theorem is satisfied when the system approaches equilibrium. For the current system described by the GP equation (1), the condition

$$2E_{\text{kin}} - 2E_{\text{pot}} + dE_{\text{int}} \simeq 0 \quad (3)$$

with d the dimension should be satisfied at equilibrium [18]. From Fig. 2, the condition $E_{\text{pot}} \simeq E_{\text{kin}} + E_{\text{int}}/2$ is indeed satisfied with $d = 1$. One can extract the equilibrium temperature T_{eq} from the equilibrium kinetic energy, $E_{\text{kin}}(t \rightarrow \infty) \equiv k_B T_{\text{eq}}/2 \simeq 364\hbar\omega$ with $T_{\text{eq}} \simeq 192$ nK.

Owing to the random nature of the wave function, it is particularly useful to study the corresponding wave-action spectrum $n_k(t)$ in the context of wave turbulence [19]. When

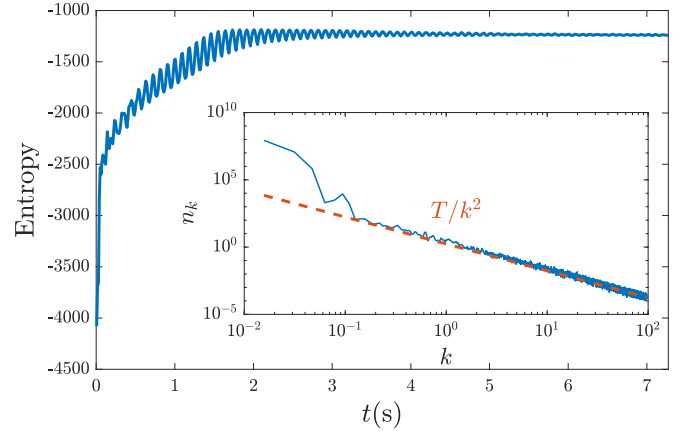


FIG. 3. Temporal entropy of the oscillating condensate calculated from the simulation in Fig. 1. The inset shows the Rayleigh-Jeans spectrum for the wave action at $t = 7.3$ s $\gg t_c$. The fitting temperature $T \simeq 192$ nK agrees with the equilibrium temperature T_{eq} extracted from the equilibrium kinetic energy shown in Fig. 2.

expressing the condensate wave function $\psi(z, t)$ in terms of Madelung transformation, $\psi(z, t) = \sqrt{\rho(z, t)} \exp[i\varphi(z, t)]$ with ρ and φ the density and phase, the hydrodynamic kinetic-energy density is $\mathcal{K} = (m/2)|(\sqrt{\rho}\mathbf{u})|^2$ with $\mathbf{u} \equiv (\hbar/m)\partial_z\varphi$ the velocity. To study the scaling laws, one applies the sum rule $\mathcal{K}(t) = \int_0^{k_c} \tilde{\mathcal{K}}(k, t) dk$, where $\tilde{\mathcal{K}}(k, t)$ is the kinetic-energy spectrum and k_c is the cutoff wave vector mentioned earlier. The corresponding wave action spectrum is then given by $n_k(t) = k^{-2}\tilde{\mathcal{K}}(k, t)$ and one can define the entropy $S(t)$ in association with n_k [20–23],

$$S(t) = \int dk \ln[n_k(t)]. \quad (4)$$

Results of $S(t)$ are shown in Fig. 3. One sees that when $t \geq 4$ s, the Fermi-Pasta-Ulam-Tsingou (FPUT) recurrence effect, that has positive correlation with the oscillation, becomes negligibly small. It confirms the onset time of localization, $t_c \sim 4$ s. Nevertheless, the entropy saturates at $t \sim 2$ s (see Fig. 3) which is earlier than t_c . It suggests that the system thermalizes first, and when thermalization has occurred, localization establishes itself in a second stage. In the inset of Fig. 3, we show n_k at $t = 7.3$ s $\gg t_c$. It follows the Rayleigh-Jeans spectrum, $n_k \simeq T/k^2$, which indicates that the energy spectrum $\tilde{\mathcal{K}}$ is a constant, or equipartition in k space. In other words, the system corresponds to a nondissipative one with a detailed balance. The fitting temperature $T \simeq 192$ nK agrees with the equilibrium temperature T_{eq} extracted from the equilibrium kinetic energy shown in Fig. 2.

Here we further discuss the onset time of localization, t_c . As studied by Bhongale *et al.* [16], by comparing the condensate center-of-mass speed v to the sound speed $c \equiv \sqrt{\mu/m}$, the entire oscillation process can be divided into fast or supersonic ($v > c$) and slow or subsonic ($v < c$) regions. When $v \leq c$, the relatively slow motion of the (central) extended part does not affect much the distribution of the (long-tail) localized part. As a matter of fact, the onset time t_c can also be interpreted as the time when the center-of-mass speed is equal to the sound speed ($v = c$). It was identified from the

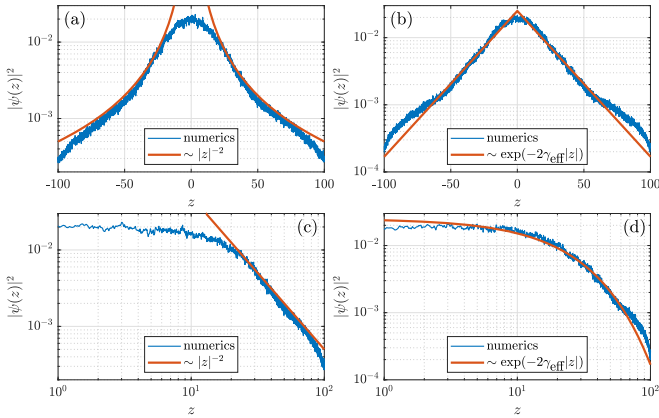


FIG. 4. (a) In a semilog plot, for the case $\xi < \sigma_D$ the eventual density distribution at $t = 7.3$ s is shown to exhibit an algebraic profile at $20 < |z| < 70$. (b) A similar study for the case $\xi > \sigma_D$, where an AL exponential profile is obtained for the eventual density distribution at $t = 3.7$ s. The fitting Lyapunov exponent is $\gamma_{\text{eff}} = 0.025$. (c),(d) The goodness of fit in (a),(b) is further confirmed by the log-log plots.

experiment [9] that $t_c \simeq 4$ s when $v = c$. This is consistent with the results shown in the temporal density profiles in Fig. 5.

In the current system of an oscillating Bose condensate in a disordered trap, the suppression of oscillations is interpreted as the onset of thermalization. In a Fermi gas in a disordered trap, Pezzé *et al.* [15,24] showed that in the weak disorder limit, the relaxation of center-of-mass oscillations is due to a dephasing between eigenmodes. It is interesting to see if the dephasing between eigenmodes can also be realized in the present Bose system. This will be considered as a future work.

Finally we investigate in detail whether a localization can be seen in the oscillation experiment. In a semilog plot, Fig. 4(a) shows the eventual spatial density distributions at $t = 7.3$ s. To smoothen the spikes arising from randomness, the results are taken as the average over a period. As shown in Fig. 4(a), it is verified that for the current $\xi < \sigma_D$ case the condensate is algebraically localized, in accordance with the previous theory [8]. As mentioned earlier, in the presence of random disorder, the condensate is actually separated into both localized and extended parts. In a free expansion experiment, the extended part will escape whereas the localized part will remain [6]. When a trapping potential is in place, the moving extended part is eventually stopped at the center of the trap, whereas the localized part comprises the long tails of the condensate. Figure 4(a) shows a well-fitting curve $|\psi(z)|^2 \sim |z|^{-2}$ at the range $20 < |z| < 70$. The lower bound is determined by the initial size of the condensate, i.e., the Thomas-Fermi radius $R_{\text{TF}} = \sqrt{2\mu} = 20$, and the off-fitting data out of the range $|z| > 70$ is due to the trapping effect. To test the goodness of fit in Fig. 4(a), an alternative log-log plot is given in Fig. 4(c).

According to Sanchez-Palencia *et al.* [8], the existence of an algebraic localization requires two conditions. First, the condensate should be in the Thomas-Fermi regime. Second, the disorder spectrum should have finite support to the

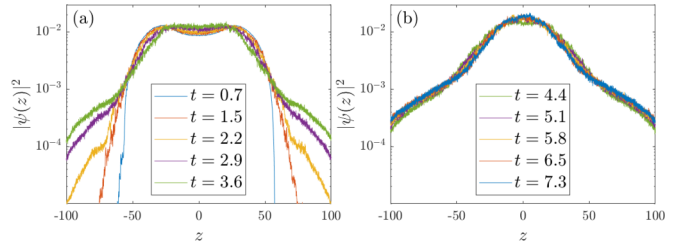


FIG. 5. Density profiles at different times obtained from the calculated results in Fig. 1. It clearly distinguishes between (a) the extended states (at $t < t_c$) and (b) the localized states (at $t > t_c$).

condensate. Our initial wave function describes a coherent condensate with a large center-of-mass velocity $v_0 = 37.5$, or a large center-of-mass kinetic energy $E_c = v_0^2/2 = 703$. When viewed from the center-of-mass coordinates, the corresponding initial kinetic energy is then $E'_{\text{kin}} = E_{\text{kin}} - E_c \simeq 705 - 703 = 2$, which is much smaller than the initial interaction energy $E_{\text{int}} \simeq 80$ (see Fig. 2). Thus our system is right in the Thomas-Fermi regime. Second, we consider the random disorder with a Gaussian-shaped disorder correlation function, thus it may not have a strict finite support to the condensate for the algebraic localization to occur. However, the parameter $\xi = 0.05$, which is five times smaller than $\sigma_D = 0.25$, so the condition of finite support is valid to a very good approximation.

As the distinction between the extended states and localized states is not convincingly shown in Fig. 1, in Fig. 5 we plot density profiles at ten different times from the calculated results in Fig. 1. Similar to Fig. 4, the results are taken as the average over a period. Figure 5 clearly shows the distinction between the extended ones (at $t < t_c$) and the localized ones (at $t > t_c$).

Can the AL be seen in a similar oscillation experiment? Here we perform another simulation for the same parameters except by reducing σ_D to 0.01 to make the regime $\xi > \sigma_D$. In this case, the onset time of localization is found to be $t_c \simeq 2$ s. As shown in Fig. 4(b), the results of the eventual density distributions at $t = 3.7$ s are well fitted by an exponential one, $|\psi(z)|^2 \sim \exp(-2\gamma_{\text{eff}}|z|)$ with γ_{eff} the Lyapunov exponent [8]. Again the goodness of fit in Fig. 4(b) is further supported by the log-log plot in Fig. 4(d). The fitting γ_{eff} is also in good agreement with the analytic one, $\gamma_{\text{eff}} = (\pi/32\xi)(V_D/\mu)^2(\sigma_D/\xi)\exp[-(\sigma_D/\xi)^2] \approx 0.025$. Compared to the case $\xi < \sigma_D$, a higher percentage of atoms can be localized in the case $\xi > \sigma_D$ as one sees that the fitting is as good as in the range $0 < |z| < 70$. The off-fitting data out of the range is again due to the trapping effect.

In summary, we propose that Anderson localization can be observed in an oscillating condensate in a disordered trap when the system comes to an equilibrium and when the healing length of the condensate exceeds the disorder correlation length. In addition, we show that in such an “isolated” system, the disorder plays the role as a medium and through it, the system undergoes a relaxation process from nonequilibrium to equilibrium. The occurrence of localization can thus be viewed as the development of thermalization in the system.

We are grateful to R. Hulet for many useful comments. Financial support from MOST, Taiwan (Grant No. MOST 105-2112-M-003-005), JSPS KAKENHI (Grant

No. 17K05548), MEXT KAKENHI/Fluctuation and Structure (Grant No.16H00807), and NCTS of Taiwan is acknowledged.

-
- [1] P. W. Anderson, *Phys. Rev.* **109**, 1492 (1958).
- [2] Y. Lahini, R. Pugatch, F. Pozzi, M. Sorel, R. Morandotti, N. Davidson, and Y. Silberberg, *Phys. Rev. Lett.* **103**, 013901 (2009).
- [3] M. Segev, Y. Silberberg, and D. N. Christodoulides, *Nat. Photon.* **7**, 197 (2013).
- [4] H. Hu, A. Strybulevych, J. H. Page, S. E. Skipetrov, and B. A. van Tiggelen, *Nat. Phys.* **4**, 945 (2008).
- [5] J. Chabé, G. Lemarié, B. Grémaud, D. Delande, P. Szriftgiser, and J. C. Garreau, *Phys. Rev. Lett.* **101**, 255702 (2008).
- [6] J. Billy, V. Josse, Z. Zuo, A. Bernard, B. Hambrecht, P. Lugan, D. Clément, L. Sanchez-Palencia, P. Bouyer, and A. Aspect, *Nature (London)* **453**, 891 (2008).
- [7] G. Roati, C. D’Errico, L. Fallani, M. Fattori, C. Fort, M. Zaccanti, G. Modugno, M. Modugno, and M. Inguscio, *Nature (London)* **453**, 895 (2008).
- [8] L. Sanchez-Palencia, D. Clément, P. Lugan, P. Bouyer, G. V. Shlyapnikov, and A. Aspect, *Phys. Rev. Lett.* **98**, 210401 (2007).
- [9] D. Dries, S. E. Pollack, J. M. Hitchcock, and R. G. Hulet, *Phys. Rev. A* **82**, 033603 (2010).
- [10] A. Polkovnikov, K. Sengupta, A. Silva, and M. Vengalattore, *Rev. Mod. Phys.* **83**, 863 (2011).
- [11] R. Nandkishore and D. A. Huse, *Annu. Rev. Condens. Matter Phys.* **6**, 15 (2015).
- [12] C. Gogolin and J. Eisert, *Rep. Prog. Phys.* **79**, 056001 (2016).
- [13] Y. P. Chen, J. Hitchcock, D. Dries, M. Junker, C. Welford, and R. G. Hulet, *Phys. Rev. A* **77**, 033632 (2008).
- [14] D. Clément, P. Bouyer, A. Aspect, and L. Sanchez-Palencia, *Phys. Rev. A* **77**, 033631 (2008).
- [15] L. Pezzé and L. Sanchez-Palencia, *Phys. Rev. Lett.* **106**, 040601 (2011).
- [16] S. G. Bhongale, P. Kakashvili, C. J. Bolech, and H. Pu, *Phys. Rev. A* **82**, 053632 (2010).
- [17] Z. Wu and E. Zaremba, *Phys. Rev. Lett.* **106**, 165301 (2011).
- [18] L. Pitaevskii and S. Stringari, *Bose-Einstein Condensation and Superfluidity* (Oxford University Press, Oxford, 2016).
- [19] S. Nazarenko, *Wave Turbulence* (Springer-Verlag, Berlin, 2011).
- [20] C. Connaughton, C. Josserand, A. Picozzi, Y. Pomeau, and S. Rica, *Phys. Rev. Lett.* **95**, 263901 (2005).
- [21] A. Picozzi, *Opt. Express* **15**, 9063 (2007).
- [22] C. Sun, S. Jia, C. Barsi, S. Rica, A. Picozzi, and J. W. Fleischer, *Nat. Phys.* **8**, 470 (2012).
- [23] M. Guasoni, J. Garnier, B. Rumpf, D. Sugny, J. Fatome, F. Amrani, G. Millot, and A. Picozzi, *Phys. Rev. X* **7**, 011025 (2017).
- [24] L. Pezzé, B. Hambrecht, and L. Sanchez-Palencia, *Europhys. Lett.* **88**, 30009 (2009).